Double-Stranded Damage of DNA·RNA Hybrids by Neocarzinostatin Chromophore: Selective C-1′ Chemistry on the RNA Strand†

Xiaoping Zeng, Zhen Xi, Lizzy S. Kappen, Weitian Tan,‡ and Irving H. Goldberg*

Department of Biological Chemistry and Molecular Pharmacology, Harvard Medical School, Boston, Massachusetts 02115

Received June 29, 1995⊗

ABSTRACT: Glutathione-activated neocarzinostatin chromophore generates bistranded lesions in the hybrid formed by yeast $tRNA^{phe}$ and DNA complementary to its 31-mer 3′ terminus. To elucidate the chemistry of the RNA cleavage reaction and to show that the lesions are double-stranded (ds), a series of shorter oligoribonucleotides containing the target sequence r(AGAAUUC)·(GAATTCT) (underlining indicates major attack site) was studied as substrates. In addition to cleavage at both U residues, major damage was produced in the form of an abasic site at the U residues. Evidence for abasic site formation on the RNA strand was obtained from sequencing-gel analysis and measurement of uracil base release. Initial evidence for the ds nature of the damage came from experiments in which 2′-*O*-methyluridine was substituted for uridine in the RNA at one or both of the target sites. The site containing the substitution was not a target for cleavage or abasic site formation, and the particular T residue, staggered two nucleotides in the 3′ direction on the complementary DNA strand, was cleaved significantly less. These studies were valuable in identifying the DNA ds partner of the RNA attack site. Direct evidence for ds lesions came from analysis of the products from a hairpin oligonucleotide construct in which the RNA and DNA strands were linked by four T residues and contained an internal ^{32}P label at the 3′ end of the RNA strand. Substitution of deuterium for hydrogen at the C-1′ position of the U residues led to a substantial isotope effect ($k_{1H}/k_{2H} = 3$) upon the formation of the RNA abasic lesion and the RNA cleavage products, providing conclusive evidence for selective 1′ chemistry. On the other hand, cleavage at the T residues on the complementary DNA strand involved C-5′ hydrogen abstraction, as was also true for the T residue in an oligodeoxynucleotide analogue of the RNA strand. Chemical mechanisms to account for the RNA cleavage and abasic site formation via C-1′ hydrogen abstraction are proposed.

The non-protein chromophore of the enediyne antitumor antibiotic neocarzinostatin (NCS-chrom) induces sequence-specific strand breaks and abasic sites in duplex DNA, following its complexation with DNA and its conversion to a diradical species upon nucleophilic attack by thiol at C-12 of the chromophore [Scheme 1; reviewed in Goldberg and Kappen (1994)]. The three-dimensional structure of the complex formed between an analogue of the glutathione-activated species of the drug and duplex DNA containing a target site has recently been elucidated (Gao et al., 1995a,b). This structure accounts for the ability of NCS-chrom to generate sequence-specific double-strand (ds) lesions. The diradical, residing in the minor groove of the DNA, is able to abstract hydrogen atoms from the C-5′, C-4′, and C-1′ positions in deoxyribose of nucleotides on the complementary strands (Scheme 2) to generate staggered oxidative lesions separated by two nucleotides in the 3′ direction. Duplex RNA has not been found to be a substrate for this reaction (Poon et al., 1977).

Recently, it has been shown that NCS-chrom can undergo general base-catalyzed activation, involving intramolecular attack of C-1″ of the naphthoate moiety on C-12 of the chromophore, to form a diradical species, which selectivity abstracts hydrogen from C-5′ at a target residue in a DNA bulge to form a strand break (Kappen & Goldberg, 1993a,b; Hensens et al., 1993, 1994). The other radical center at C-2 is quenched intramolecularly by C-8″ of the naphthoate moiety only in the presence of the bulged DNA substrate. This reaction results in highly efficient site-specific cleavage in the absence of thiol at a single nucleotide at the 3′ side of the bulge in single-stranded (ss) DNAs that are capable of folding into hairpin structures, as well as in related bulge-containing duplex DNAs made up of two linear complementary oligomers. Recently, this reaction has also been found to occur in the bulge region of the transactivation response region RNA (TAR) of HIV-1 and its DNA analogue (Kappen & Goldberg, 1995). The cleavage in the TAR bulge was significantly weaker than that in the bulge of its DNA analogue, which involved 4′ as well as 5′ chemistry.

Scheme 1: Thiol Activation of NCS-Chrom to the Diradical Species

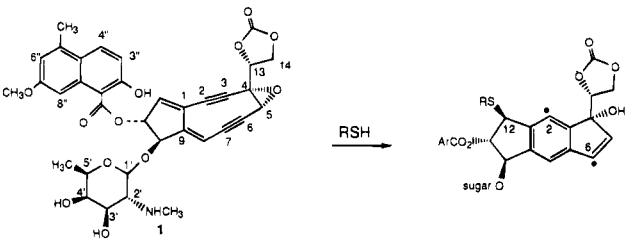

To date, the reported damage induced by thiol-activated NCS-chrom has been limited to B-type duplex DNA; lesions occurring in ss DNA has been attributed to the formation of

† This work was supported by U.S. Public Health Service Grant CA44257 from the National Institutes of Health.

* Author to whom correspondence should be addressed.

‡ Current address: Hybridon Inc., 1 Innovation Dr., Worcester, MA 01605.

⊗ Abstract published in *Advance ACS Abstracts,* September 15, 1995.

0006-2960/95/0434-12435$09.00/0

Scheme 2: Proposed Mechanism of NCS-Induced DNA Damage at C-1′, C-4′, and C-5′

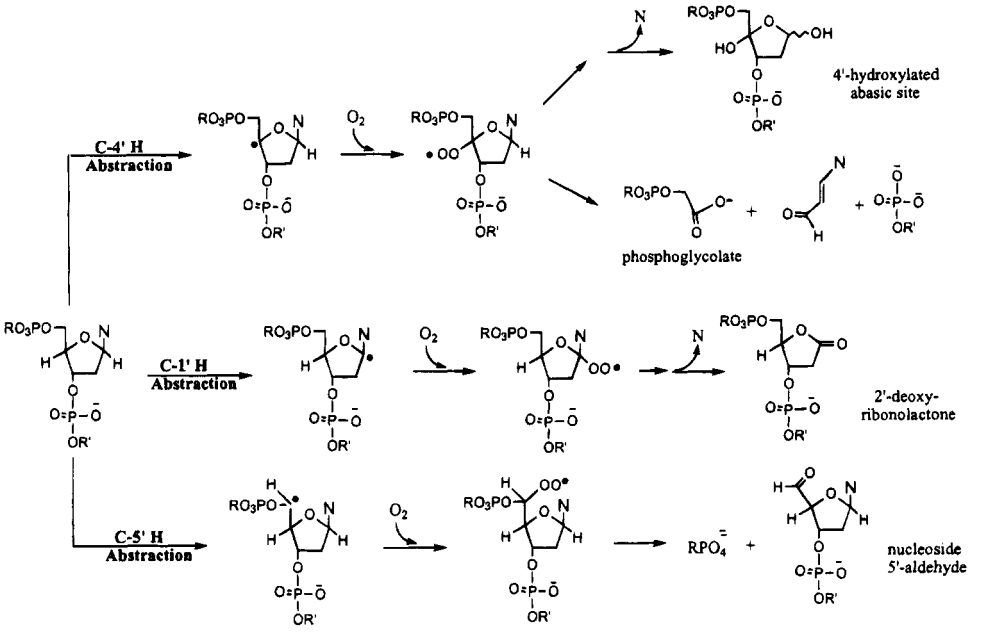

ds regions. As part of an effort to extend the utility of enediynes as tools in the study of unusual nucleic acid structures, it was of interest to determine whether NCS-chrom, thiol- or base-activated, produced lesions in DNA·RNA hybrids of presumed A type conformation. Although it was reported some years ago that the DNA·RNA hybrid composed of poly(dT)·poly(rA) protected against the cleavage of λ phage DNA by thiol-activated neocarzinostatin (Poon et al., 1977), possible damage in the hybrid itself has not been explored. We now present direct evidence that glutathione-activated NCS-chrom generates staggered ds lesions in DNA·RNA hybrids, involving C-1′ hydrogen abstraction from the targeted ribonucleotide and C-5′ chemistry at the targeted deoxyribonucleotide. By contrast, the lesions generated on a DNA analogue (DNAa) of the RNA strand (in a DNA·DNAa duplex) involves C-5′, not C-1′, chemistry.

MATERIALS AND METHODS

Neocarzinostatin was obtained from Kayaku Antibiotics (Tokyo). NCS-chrom was extracted from the holoantibiotic with cold methanol in the presence of citrate (Kappen & Goldberg, 1985). Commercial ribonucleoside phosphoramidites were from Glen Research. 2′-*O*-Methylphosphoramidites were from Chem-Genes (Needham, MA). [5,6-^{3}H]-UTP (13.7 Ci/mmol), [γ-^{32}P]ATP (3000 Ci/mmol), and [5′-^{32}P]pCp (3000 Ci/mmol) were from New England Nuclear DuPont, and [5-^{3}H]CTP (21 Ci/mmol) was from ICN. T4 polynucleotide kinase, T7 RNA polymerase, and RNA Sequencing Kit were from United States Biochemical (USB). T4 RNA ligase and calf intestinal alkaline phosphatase were from New England Biolabs.

Synthesis of 5′-Dimethoxy-5′-deuterio-2′-O-TBDMS-uridine 3′-Cyanoethyl Phosphoramidite. The deuterium at the C-1′ position of ribose was introduced by diisobutylaluminium deuteride reduction of γ-D-ribonolactone (98% incorporation of deuterium selectively at C-1′ as determined by 500 MHz NMR). The uridine ribonucleoside was synthesized by Vorbrüggen's procedure (Vorbrüggen & Bennua, 1981). The phosphoramidite derivative was prepared by 5′-tritylation and 2′-silylation followed by 3′-phosphorylation of 1′-deuteriouridine (Khare & Orban, 1992).

Synthesis of Oligonucleotides. Oligonucleotides were made by solid-phase synthesis using an Applied Biosystems 381A DNA synthesizer (Herschlag et al., 1993). The following RNA oligonucleotides were synthesized by the DNA synthesizer: R17, CACAGAAUUCGCACCAG; R11, CACAGAAUUCG, CACAGAAU$_8$*UCG (U$_8$*, [1′-^{2}H]uridine), CACAGAAU$_8$*U$_9$*CG (U$_8$* and U$_9$*, [1′-^{2}H]uridine); CACAGAAU$_{OMe}$UCG (U$_{OMe}$, 2′-*O*-methyluridine); CACAGAAUU$_{oMe}$CG; CACAGAAU$_{OMe}$U$_{OMe}$CG; and the hairpin RNA·DNA oligonucleotide r(CACAGAAUUCG)d(TTTTCGAATTCTGTG). RNA oligonucleotides (R14, pGGGAGGAGAAUUCG) containing the ^{3}H label were synthesized by transcription using T7 RNA polymerase (Milligan et al., 1987). The transcripts, containing predominantly 5′-monophosphate ends, were obtained using a GMP to GTP ratio of 10:1 (Strobel & Cech, 1993).

^{32}P End Labeling and Sequencing. Labeling of oligonucleotides at the 5′ end was achieved by T4 polynucleotide kinase and [γ-^{32}P]ATP. The oligonucleotides made by T7 RNA polymerase were dephosphorylated of their 5′-phosphate ends by calf intestinal alkaline phosphatase, purified by 20% sequencing gel, and then 5′-end-labeled. 3′end labeling using T4 RNA ligase and [5′-^{32}P]pCp was as described (England et al., 1980). The 3′-end-labeled oligonucleotides were dephosphorylated by calf intestinal alkaline phosphatase prior to purification by 20% sequencing gels. Sequencing of the ^{32}P-end-labeled RNA oligonucleotides was carried out enzymatically by using the RNA sequencing kit (USB) and a chemical method (Peattie, 1979).

Preparation of Internal ^{32}P-Labeled Hairpin Oligonucleotides and Hairpin Oligonucleotide Fragments. Hairpin oligonucleotide r(CACAGAAUUCG^{32}$_p$)d(TTTTCGAATTCTGTG$_p$) was prepared by ligation of RNA oligonucleotide CACAGAAUUCG with 5′-^{32}P-end-labeled oligodeoxyribonucleotide ^{32}$_p$TTTTCGAATTCTGTG$_p$ using T4 RNA ligase. 5′-^{32}P-end-labeled oligodeoxyribonucleotide ^{32}$_p$TTTTC-

GAATTCTGTG$_p$ was obtained by treatment of 5′-^{32}P-end-labeled oligonucleotide d(^{32}$_p$TTTTCGAATTCTGTG)rC with sodium periodate and aniline (Steinschneider & Fraenkel-Conrat, 1966). Oligonucleotide d(TTTTCGAATTCTFTG)rC was synthesized by the DNA synthesizer with rC-CPG and 5′-^{32}P-end-labeled with T4 polynucleotide kinase. Hairpin oligonucleotides containing deuterium isotope ($\underline{U}_8$* and $\underline{U}_9$*, [1′-^{2}H]uridine) were made by the same strategy, except that RNA oligonucleotides CACAGAA$\underline{U}_8$*UCG and CACAGAA$\underline{U}_8$*$\underline{U}_9$*CG were employed for the ligation. Hairpin oligonucleotide fragments r(CACAGAAUUCG^{32}$_p$)d(TTTTCGAA$_p$) and r(CACAGAAUUCG^{32}$_p$)d(TTTTCGAAT$_p$) were prepared from d(TTTTCGAA)rC and d(TTTTCGAAT)rC, respectively.

NCS-Chrom Reaction. Reactions for cleavage of the yeast tRNA^{phe} 31-mer DNA (complementary to residues 46−76 of tRNA^{phe}) hybrid contained 50 mM Tris-HCl (pH 7.5), 1 mM EDTA, 1 mM glutathione, tRNA^{phe}, 31-mer, and NCS-chrom at the concentrations given in Figure 1. All reactions contained 10% methanol. Prior to the addition of glutathione and NCS-chrom, the mixture was annealed by heating at 90 °C for 2 min followed by slow cooling. NCS-chrom was added last. The reaction proceeded for 1 h at room temperature in the dark. Samples were dried in a Speed-Vac concentrator, resuspended in loading solution (80% formamide and 1 mM EDTA), and analyzed on 15% sequencing gels.

Standard reactions for the DNA·RNA oligonucleotide hybrids or DNA·DNA oligonucleotide duplex were carried out in a volume of 30 μL containing 20−40 mM Tris-HCl (pH 8.0), RNA·DNA or DNA·DNA oligonucleotides, NCS-chrom, and glutathione. The reaction was initiated by the addition of NCS-chrom or thiol and proceeded for 1 h in ice in the dark. The final concentrations of RNA oligonucleotide, DNA oligonucleotide, glutathione, and NCS-chrom are indicated in the figure legends. Additional treatments of NCS-chrom-treated DNA oligonucleotide with sodium borohydride, sodium hypoiodite, hydrazine, and piperidine were carried out as described (Kappen & Goldberg, 1983, 1992; Kappen et al., 1991). Standard reaction for the hairpin DNA·RNA oligonucleotide contained internal ^{32}P-labeled hairpin RNA·DNA oligonucleotide (60 000 cpm, 28 μM nucleotide), 16 mM Tris-HCl (pH 8.0), 21 μM NCS-chrom, and 1 mM glutathione. The reaction was initiated by the addition of NCS-chrom and allowed to proceed in ice in the dark for 2 h. Samples were dried in a Speed-Vac concentrator, resuspended in 80% formamide loading solution, and analyzed on 20% sequencing gels.

Isolation and Sequencing of **11a**. Product **11a** was generated in the reaction containing 5′-^{32}P-end-labeled R11 (10 μM nucleotide), the complementary oligodeoxyribonucleotide (45 μM nucleotide), 40 mM Tris-HCl (pH 8.0), 37 μM NCS-chrom, and 1 mM glutathione in a volume of 30 μL. After a 1 h reaction in ice in the dark, the sample was dried in a Speed-Vac concentrator, resuspended in 80% formamide loading solution, and analyzed on a 20% sequencing gel. Band **11a** was excised from the gel and eluted overnight at 4 °C in 0.15 M sodium acetate (pH 7.0) and 1 mM EDTA. After removal of the gel, the solution was desalted using a Sep-Pak reverse-phase cartridge. The product was eluted with 50% methanol in H_2O and dried in a Speed-Vac concentrator. The isolated **11a** was sequenced using the RNA sequencing kit (USB).

Base Release. In order to determine NCS-chrom-induced base release, oligoribonucleotides having the ^{3}H label at $\underline{U}$ residues or at a $\underline{C}$ residue and ^{32}P at their 5′ ends were used as substrates. A typical reaction (1 h in ice) contained 5′-^{32}P-end-labeled RNA oligonucleotide $_p$GGGAGGAGAA-$\underline{UU}$CG ($\underline{U}$ [5,6-^{3}H]uridine, 2 μM, ^{3}H, 2.1 × 10^6 cpm), the complementary DNA oligonucleotide (3 μM), 20 mM Tris-HCL (pH 8.0), 37 μM NCS-chrom, and 0.5 mM glutathione in a volume of 60 μL and was allowed to proceed for 1 h in ice in the dark. After the addition of 5 μg of tRNA as carrier, the oligonucleotides were precipitated by ethanol (75%), resuspended in 80% formamide loading solution, and then loaded on a 20% sequencing gel. The bands of original starting materials and **14a** were excised and eluted in 0.15 M sodium acetate (pH 7.0) and 1 mM EDTA. The radioactivity in the eluate was determined by liquid scintillation counting. The supernatant of the 75% ethanol precipitation containing 4.4 × 10^5 cpm of ^{3}H was concentrated to 50 μL in a Speed-Vac, and 5 μL of this sample was analyzed by thin-layer chromatography (TLC) in two different solvent systems, ethyl acetate/isopropyl alcohol/H_2O (74:17:9) and ethanol/1 M sodium acetate (7:3). The radioactivity in 1 cm strips of TLC and in the gel eluate was determined by liquid scintillations counting.

Quantitation of Damaged Products. The damaged products generated by NCS-chrom were separated by 20% sequencing gels and quantified by using a Molecular Dynamics PhosphorImager with Image Quant software version 3.22 or an LKB Ultroscan XL laser densitometer.

RESULTS AND DISCUSSION

Sequence-Specific Cleavage of a Hybrid Containing tRNA^{phe} and DNA. Treatment of 3′-end-labeled tRNA^{phe} that had been annealed with 31-mer DNA (complementary to residues 47−76 of tRNA^{phe}) with NCS-chrom in the presence of glutathione generates discrete cleavage bands (lane 2, Figure 1A). No cleavage by the drug is observed in the hybrid in the absence of glutathione (lane 3) or with tRNA^{phe} alone in the presence of glutathione (lane 4). The strand cleavage in the hybrid is confined to the AAUUC sequence region, with U_{68} and U_{69} being more strongly attacked than the A residues and C. The experiments in Figure 1B were designed to examine the damage in the DNA strand of the hybrid. Treatment of the hybrid containing 5′-^{32}P-end-labeled 31-mer DNA induces strong cleavage at T_{10} and T_{11} (lane 1, Figure 1B). This is in contrast to the expected pattern of cleavage at mainly T's and A's in the Watson−Crick base-paired 31-mer DNA (lane 3). A histogram representation of the sequence-specific cleavage of the tRNA^{phe}·DNA hybrid is shown in Figure 1C. The cleavage of U_{69} is stronger than that at U_{68}, corresponding to the cleavage at T_{10} being stronger than that at T_{11} (lane 2, Figure 1A; lane 1, Figure 1B). Major cleavages appear to involve two ds cleavage sites at the sequences r(AA$\underline{U}_{68}$)·d(AT$\underline{T}_{11}$) and r(AU$\underline{U}_{69}$)·d(AA$\underline{T}$) (cleavage sites shown underlined). The two-base-pair stagger in the 3′ direction of the hybrid lesions is the same as that found earlier for ds lesions in duplex DNA (see Goldberg, 1991), implicating ds attack from the minor groove. Since the cleavages at T sites are stronger than those at the U sites (lane 2, Figure 1A; lane 1, Figure 1B), it is suggested that ss lesions are also found at the T sites, in addition to their involvement in ds lesions.

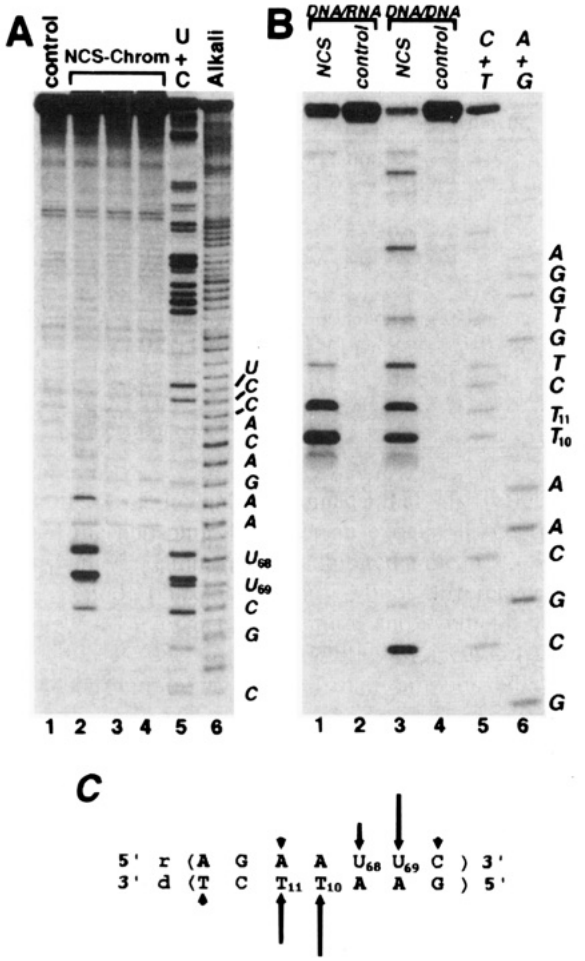

FIGURE 1: Sequence-specific cleavage of tRNA^{phe} and complementary 31-mer DNA in the hybrid. (A) 3′-^{32}P-end-labeled tRNA^{phe} (900 μM nucleotide), either alone or after annealing with its complementary 3′ terminal 31-mer DNA (122 μM nucleotide), was treated with NCS-chrom (48 μM) under standard reaction conditions given in Materials and Methods: lane 1, RNA with no NCS-chrom; lane 2, RNA·DNA hybrid treated with NCS-chrom in the presence of glutathione; lane 3, RNA·DNA hybrid treated with NCS-chrom in the absence of glutathione; lane 4, RNA alone treated with NCS-chrom in the presence of glutathione; lane 5, chemical sequencing lane, U > C; lane 6, alkali-induced cleavage of RNA. (B) NCS-chrom-induced cleavage in the DNA strand. In reactions similar to those in (A), 31-mer DNA carried the ^{32}P label at its 5′ end: lanes 1 and 2, 31-mer DNA was annealed with tRNA^{phe}; lanes 3 and 4, 31-mer annealed to its complementary DNA strand; lanes 5 and 6, Maxam−Gilbert sequencing, C+T and A+G, respectively. (C) Histogram of NCS-chrom-mediated cleavage of RNA·DNA hybrid summarized from (A) and (B). Major cleavage sites are indicated by arrows. The length of the arrows is approximately proportional to the intensity of cleavage.

NCS-Chrom-Mediated Damage of the RNA Strand of the RNA·DNA Oligonucleotide Hybrids. In order to determine whether the glutathione-activated NCS-chrom can specifically cleave DNA·RNA hybrids at the sequence r(AGAAUUC)·dGAATTCT), and to explore the mechanism of the hybrid damage, we synthesized RNA oligonucleotides containing the AGAAUUC sequence and their complementary DNA oligonucleotides. As shown in Figure 2A,B, the NCS-chrom-mediated damage of 3′-^{32}P-end-labeled R11 (lane 2, Figure 2A) and 3′-^{32}P-end-labeled R17 (lane 3, Figure 2B) produces two cleavage products from each substrate that comigrate with the fragments formed by U-specific sequencing. The cleavage products are 5′-phosphate-ended since their mobilities are identical to that

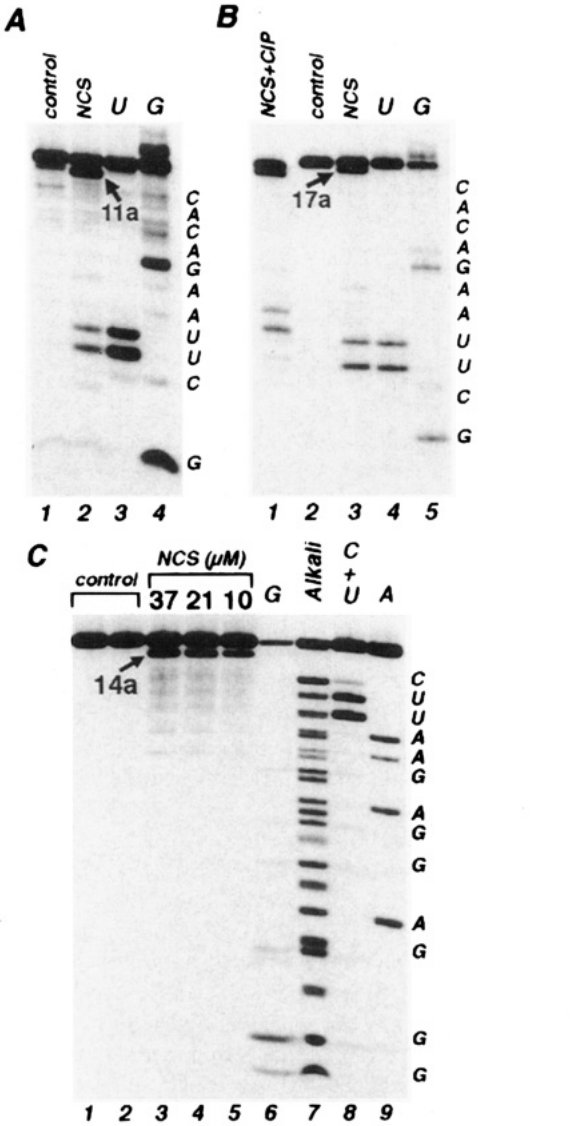

FIGURE 2: NCS-chrom-mediated damage of RNA·DNA hybrids. (A) Damage of 3′-^{32}P-end-labeled R11 CACAGAAUUCG$^{32}_{p}$C (10 μM nucleotide): lane 2, RNA·DNA oligonucleotides (ratio 1:4.8) were treated with 37 μM NCS-chrom in the presence of 1 mM glutathione; lane 1, no glutathione control; lanes 3 and 4, chemical sequencing lanes, U and G. (B) Damage of 3′-^{32}P-end-labeled R17 CACAGAAUUCGCACCAG$^{32}_{p}$C (21 μM nucleotide): lane 3, RNA·DNA oligonucleotides (ratio 1:4.8) were treated with 21 μM NCS-chrom in the presence of 1 mM glutathione; lane 2, no glutathione control; lane 1, portion of the reaction mixture was treated with calf intestinal alkaline phosphatase (CIP); lanes 4 and 5, chemical sequencing lanes U and G. (C) Damage of 5′-^{32}P-end-labeled R14 GGGAGGAGAAUUCG (10 μM nucleotide). RNA·DNA oligonucleotides (ratio 1:5.8) were treated with 37, 21, and 10 μM NCS-chrom (lanes 3−5) in the presence of 1 mM glutathione; lanes 2, 37 μM NCS-chrom but no glutathione; lane 1, no NCS-chrom control; lanes 6−9, sequencing lanes using RNA sequencing kit (USB).

of the U marker and are made significantly slower by treatment with calf intestinal alkaline phosphatase (lane 1, Figure 2B), presumably due to the removal of the 5′-phosphate end. In addition, there are two major damage products **11a** and **17a** from R11 and R17, respectively, which have mobilities slightly faster than those of the starting materials (Figure 2A,B), suggesting the presence of an abasic site (Kappen et al., 1988). Figure 2C shows the damage of 5′-^{32}P-end-labeled R14 annealed with its complementary DNA strand, producing **14a** with a slightly faster mobility

```
R11-D17     CACAGAAUUCG
            gtgtcttaagcgtggtc

R11-D12     CACAGAAUUCG
            gtgtcttaagcg

R11-D11     CACAGAAUUCG
            gtgtcttaagc

R11-D10     CACAGAAUUCG
            gtgtcttaag

R11-D9      CACAGAAUUCG
            gtgtcttaa

R11-D8      CACAGAAUUCG
            gtgtctta

R11-D7      CACAGAAUUCG
            gtgtctt

R11-D7'     CACAGAAUUCG
                cttaagc
```

FIGURE 3: RNA·DNA oligonucleotide sequences: RNA oligonucleotide, upper case; DNA oligonucleotide, lower case.

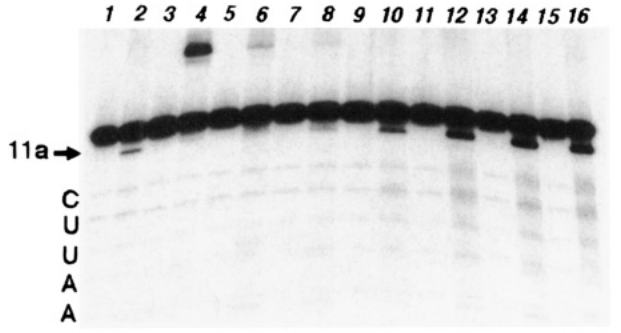

FIGURE 4: Effect of varying DNA oligonucleotide lengths in the hybrid on the damage of 5′-^{32}P-end-labeled R11 CACAGGUUCG (28 μM nucleotide). RNA·DNA oligonucleotides (ratio 1:6.5) were treated with 24 μM NCS-chrom in the presence of 0.75 mM glutathione: lane 2, R11-D7′; lane 4, R11-D7; lane 6, R11-D8; lane 8, R11-D9; lane 10, R11-D10; lane 12, R11-D11; lane 14, R11-D12; lane 16, R11-D17; lanes 1, 3, 5, 7, 9, 11, 13, and 15, no NCS-chrom control for lanes 2, 4, 6, 8, 10, 12, 14, and 16, respectively.

(lanes 3−5) than R14. No other cleavage product is clearly shown for this 5′-^{32}P-end-labeled substrate except for a faint series of bands and an interband smear in the sequencing marker UUC region, suggesting the breakdown of a product with a labile moiety at its 3′ end. The breaks at U in Figure 2A,B are consistent with the previous results using 3′-end-labeled tRNA^{phe} (Figure 1A). The absence of a distinct band with a faster mobility than the starting material in the later case can be explained by the relatively poor resolution obtained with the much longer tRNA in this region of the gel.

Effect of Varying DNA Oligonucleotide Lengths in the Hybrids on Damage. To test whether the length of the complementary DNA oligonucleotide affects the formation of **11a**, DNA·RNA oligonucleotide hybrids shown in Figure 3 were used as substrates for NCS-chrom. As shown in Figure 4, the damage of 5′-^{32}P-end-labeled R11 produces a substantial amount of **11a** in the presence of its complementary DNA strand, 11-mer or longer (lanes 12, 14, and 16). As noted in lane 4, where the UUCG region of R11 is not base-paired, and in lanes 6 and 8, where base-pairing is incomplete, **11a** is either absent or decreased, with the appearance of an unidentified product (possibly an adduct or a cross-linked structure) moving much more slowly than the 5′-^{32}P-end-labeled R11. Interestingly, the amount of the

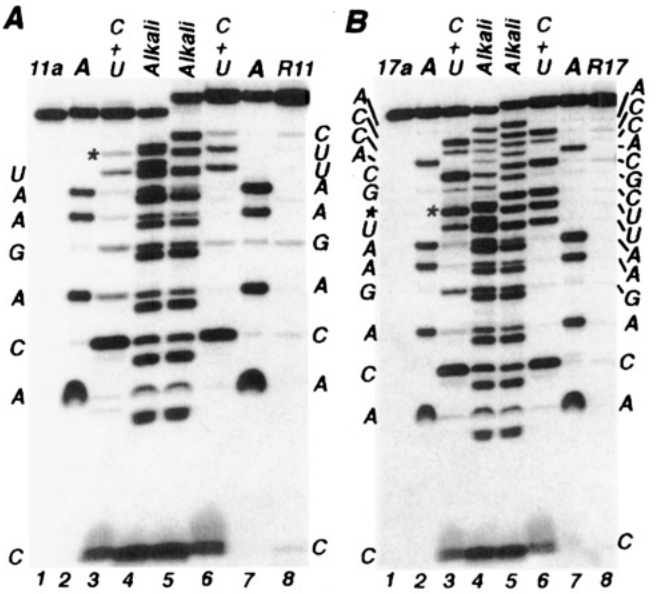

FIGURE 5: (A) Sequencing of 5′-^{32}P-end-labeled R11 CACAGAAUUCG (lanes 1−4) and **11a** (lanes 5−8) isolated from NCS-chrom-treated, 5′-^{32}P-end-labeled R11, as described in Materials and Methods. (B) Sequencing of 5′-^{32}P-end-labeled R17 CACAGAAUUCGCACCAG (lanes 1−4) and **17a** (lanes 5−8) isolated from NCS-chrom-treated, 5′-^{32}P-end-labeled R17. Asterisks are described in the text.

unidentified product varies inversely with that of **11a**. In contrast to the finding in lane 4, the complementary DNA oligonucleotide of the same length (7-mer) that base-pairs with this region produces a small amount of **11a** (lane 2). Clearly, **11a** formation is dependent on the stability of the hybrid, inclusive of the targeted sequence. A smear in the UUC region is observed in lanes 12, 14, and 16 for the 5′-^{32}P-end-labeled R11, similar to the finding in Figure 2C.

Sequencing of **11a** *and* **17a**. 5′-^{32}P-end-labeled **11a** and **17a** were subjected to enzymatic sequencing to determine the lesion site. Compared with the sequencing of R17, the sequencing of **17a** reveals an anomolous mobility pattern in fragments longer than that indicated by an asterisk (Figure 5B). In Figure 5B, when the bands in the two alkali treatment lanes 4 and 5 are identified from the top to the bottom of the sequence marked ACCACG, the corresponding fragments of **17a** are found to move faster than those of R17 suggesting that they contain an abasic site. Fragments containing an abasic site are known to move faster than their parent oligonucleotides (Kappen et al., 1988). The bands with asterisks in Figure 5A,B could be generated by enzymatic cleavage at either C or U: the former would have to contain an abasic site. The results with sequencing **11a** are consistent with this interpretation.

Base Release. To determine directly that an abasic site was generated in the drug-treated reaction, and to identify the particular base involved, a 14-mer RNA oligonucleotide containing ^{3}H-labeled base residues at both U_{11} and U_{12} or at C_{13} was used as substrate. The previous sequencing data (vide supra) appeared to implicate one or more of these bases in possible abasic site formation. Figure 6A shows that a significant amount of free labeled uracil was present in the supernatant, resulting from ethanol precipitation of the NCS-chrom-treated, 5′-^{32}P-end-labeled RNA GGGAGGAGAA-UUCG (U, [5,6-^{3}H]uridine). As shown in Figure 6B, the amount of cytosine released from the treatment of 5′-^{32}P-end-labeled RNA GGGAGGAGAAUUCG (C, [5-^{3}H]cyti-

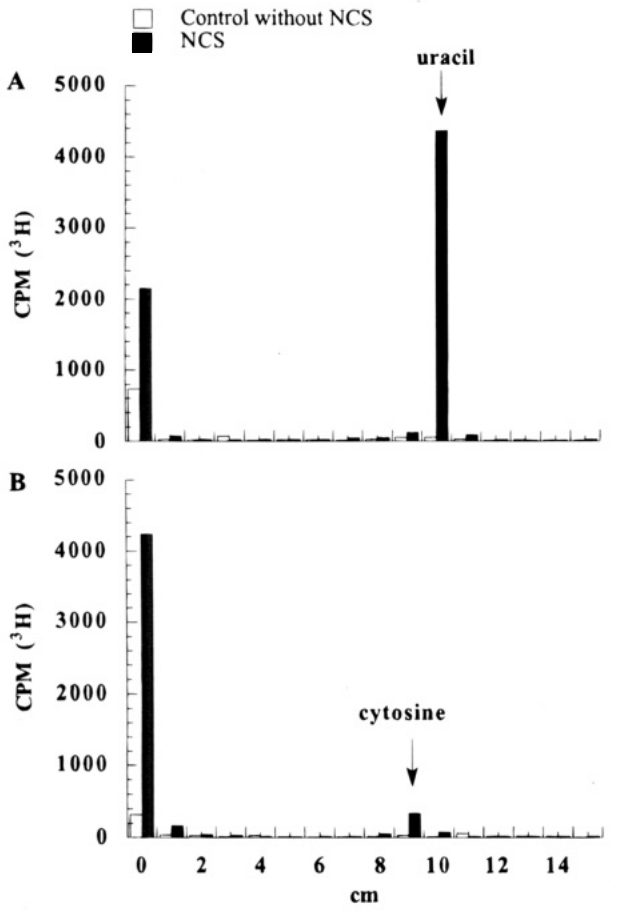

FIGURE 6: Thin-layer chromatographic analysis of NCS-chrom-mediated free base release. Silica gel TLC plates were developed in a solution of ethanol and 1 M sodium acetate (7:3). (A) NCS-chrom-mediated damage of the 14-mer RNA GGGAGGAGAA**UU** (**U**, [5,6-^{3}H]U). (B) NCS-chrom-mediated damage of the 14-mer RNA GGGAGGAGAAUU**C**G (**C**, [5-^{3}H]C). Arrows indicate the positions of authentic uracil and cytosine.

dine) under the same experimental conditions is minor. The ^{3}H was found to comigrate with uracil in two different solvent systems (data not shown). To examine whether the free uracil is coproduced with **14a**, we separated **14a** from the starting material by sequencing-gel electrophoresis and eluted both. The eluant containing **14a** has the ratio ^{3}H:^{32}P = 1.31, while that of the starting material has the ratio 2.39. A 45% ^{3}H loss resulted from NCS-chrom treatment of GGGAGGAGAA**UU**CG (**U**, [5,6-^{3}H]uridine) in the formation of **14a**. If only one abasic site per molecule is formed, the ^{3}H loss from one **U** can account for 90% of **14a** formation.

Effect of 2′-O-Methyl Substitution on DNA·RNA Hybrid Damage. Substitution of uridine with 2′-*O*-methyluridine in R11 significantly affects RNA·DNA oligonucleotide hybrid damge. As shown in Figure 7A, NCS-chrom-induced damage of R11 products **11a** and two fragments resulting from the cleavage of R11 at U_8 (weaker) and U_9 (stronger) (lane 1). Interestingly, when U_8 is replaced by 2′-*O*-methyluridine, there is no cleavage at U_8 but other damaged products are more or less the same (lane 3, Figure 7A). Further when U_9 was replaced by 2′-*O*-methyluridine, the cleavage at U_9 is significantly reduced and **11a** also appears less (lane 4, Figure 7A). Finally, the damage of the R11 mutant is no longer apparent when both uridines are replaced by 2′-*O*-methyluridine (lane 2, Figure 7A). From this experiment, we can conclude that **11a** consists of an abasic

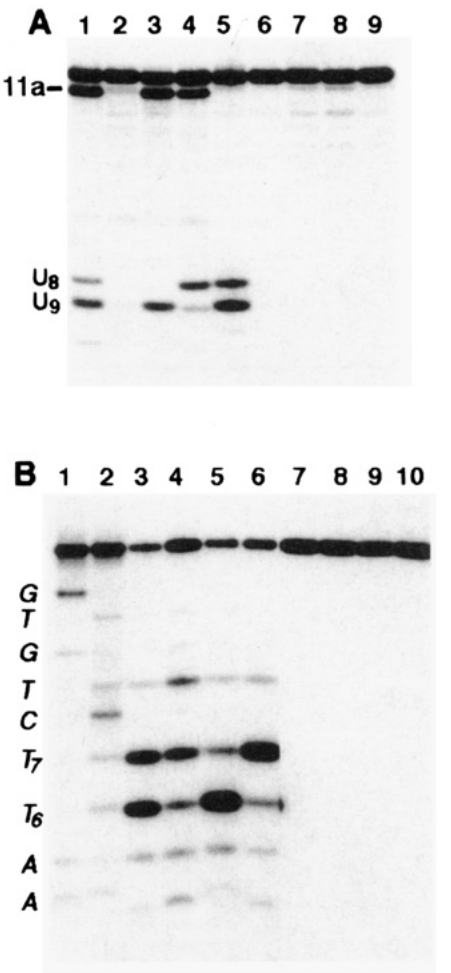

FIGURE 7: (A) Effect of 2′-*O*-methyluridine substitution in RNA oligonucleotides on NCS-chrom-induced damage in DNA·RNA hybrids: lane 1, treatment of 3′-^{32}P-end-labeled R11 CACAGAAUUCG^{32}$_p$C (9.6 μM nucleotide) with 37 μM NCS-chrom in the presence of its complementary oligodeoxyribonucleotide (40 μM nucleotide) and 1 mM glutathione; lanes 2−4, same as in lane 1 except 3′-^{32}P-end-labeled RNA oligonucleotide mutants CACAGAAU$_{OMe}$U$_{OMe}$CG^{32}$_p$C, CACAGAAU$_{OMe}$UCG^{32}$_p$C, and CACAGAAUU$_{OMe}$CG^{32}$_p$C, respectively, were in the hybrids; lane 5, chemical sequencing, U; lanes 5−9, no NCS-chrom control for lanes 1−4, respectively. (B) Cleavage of 5′-^{32}P-end-labeled oligodeoxyribonucleotide GCGAATTCTGTG (51 μM nucleotide). DNA·RNA oligonucleotides (regular R11 or RNA oligonucleotide mutants, 114 μM nucleotide) were treated with 21 μM NCS-chrom in the presence of 1 mM glutathione; lane 3, regular R11; lane 4, CACAGAAU$_{OMe}$U$_{OMe}$CG; lane 5, CACAGAAU$_{OMe}$UCG; lane 6, CACAGAAUU$_{OMe}$CG; lanes 1 and 2, Maxam−Gilbert sequencing, G+A and C+T, respectively; lanes 7−10, no NCS-chrom control for lanes 3−6, respectively.

site at U_8 or U_9, but not at both in the same molecule. Further, the **11a** in lane 3 and the **11a** in lane 4 (Figure 7A) are caused by U_9 damage and U_8 damage, respectively, since the site containing 2′-*O*-methyluridine is a very poor target, as shown in lane 2. Figure 7B shows cleavage of the DNA in the hybrid having a complementary RNA oligonucleotide containing 2′-*O*-methyluridine. In comparison with the hybrid containing U residues (lane 3), 2′-*O*-methyluridine substitution at U_8 results in inhibition of cleavage at T_7 (lane 5), while that at U_9 inhibits cleavage at T_6 (lane 6). Substitution at both U sites in the RNA inhibits cleavage at both T_7 and T_6 (lane 4), although significant ss cleavage remains at the former site. These results clearly imply that the presence of a 2′-*O*-methyl substituent at one U site on the RNA strand results in inhibition of cleavage at its ds

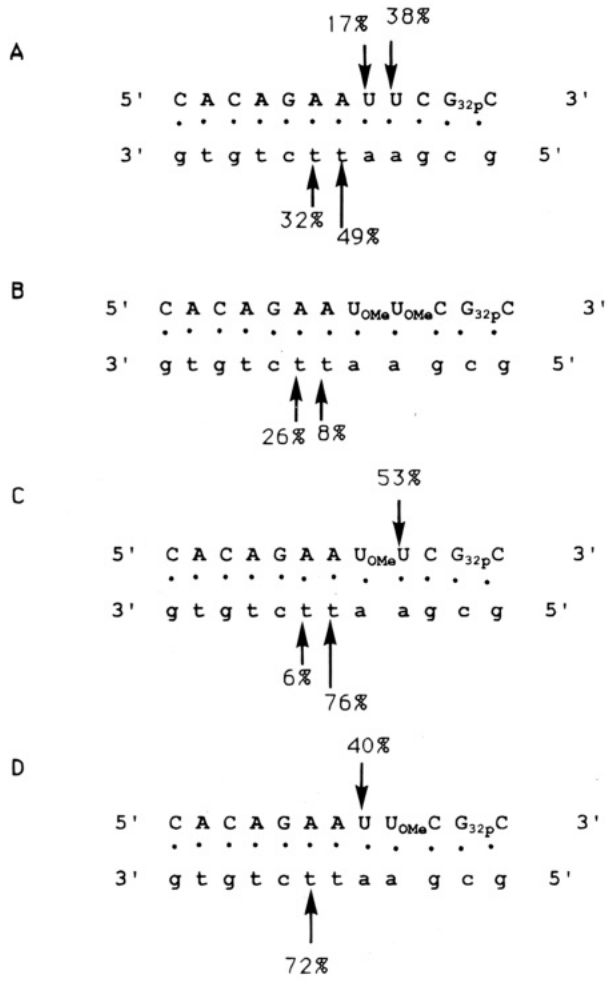

FIGURE 8: Summary of the effect of 2′-*O*-methyluridine substitution in RNA oligonucleotide on the damage of RNA·DNA hybrids. The arrows indicate the sites of damage quantified from Figure 7. As described in the text, the percent damage in **11a** due to abasic site formation at a specific U residue was calculated from the ratio of cleavage at these sites. The percent cleavage at the T residues was directly determined. Cleavage below 5% is not shown.

partner on the complementary strand, thus permitting identification of the ds partner target site.

Figure 8 summarizes the results of Figure 7. Calculation of the percent damage at the particular RNA target site was based on the assumption that the ratio of cleavage at U_8 and U_9 also reflects their respective attack frequencies in **11a** formation. As shown in Figure 8A, major damage in the sequence r(AA$\underline{U}_8\underline{U}_9$)·d(AA$\underline{T}_6\underline{T}_7$) appears to consist of two ds cleavage sites in the sequences r(AA$\underline{U}_8$)·d(AT$\underline{T}_7$) and r(AU$\underline{U}_9$)·d(AA$\underline{T}_6$) (cleavage site shown underlined), consistent with the behavior of the tRNA^{phe}·DNA hybrid in Figure 1. The cleavage at $\underline{U}_9$ is stronger than that at $\underline{U}_8$; correspondingly, $\underline{T}_6$ cleavage is stronger than that at $\underline{T}_7$. One ds cleavage site is diminished when one uridine is replaced by one 2′-*O*-methyluridine, as shown in Figure 8C,D. The finding that cleavage at the $\underline{T}$ sites of the DNA strand is stronger than that at the U sites of the RNA strand (Figure 8) suggests that some of the breaks at T's are not involved in the ds lesion and are due to ss cleavage. Figure 8B shows ss cleavage at T_7 (stronger) and T_6 (weaker) when the two uridines are replaced by two 2′-*O*-methyluridines.

The presence of an abasic site in DNA can be readily confirmed by alkali treatment, which selectively cleaves the DNA at the lesion. However, alkali treatment is not

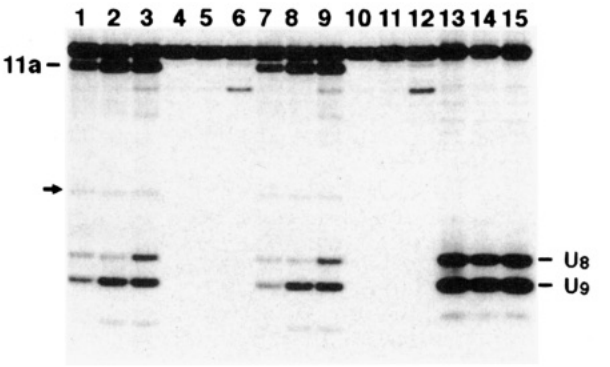

FIGURE 9: Deuterium isotope effect on U site damage by NCS-chrom. 3′-^{32}P-end-labeled R11 CACAGAAUUCG$^{32}_{p}$C (8.5 μM nucleotide) and its complementary oligodeoxyribonucleotide (40 μM nucleotide) were treated with 21 μM NCS-chrom in the presence of 1 mM glutathione; in lanes 1−3, glutathione was added last to start the reaction. In lanes 7−9, NCS-chrom was added last: lanes 3 and 9, R11 (U_8 and U_9, 1′-^{1}H); lanes 2 and 8, $\underline{U}_8$* ($\underline{U}_8$*, 1′-^{2}H); lanes 1 and 7, $\underline{U}_8$*$\underline{U}_9$*, 1′-^{2}H); lanes 4, 5, 6, 10, 11, and 12, no NCS-chrom control for lanes 1, 2, 3, 7, 8, and 9; lanes 13−15, U-specific chemical sequencing for the preceding three substrates. Arrow indicates the band taken for the normalization of data in different lanes for calculation of the isotope effect.

applicable to such a lesion in RNA due to the extensive degradation of the RNA. The 2′-*O*-methyl substituent favors the same $C_{3'}$-endo sugar conformation as does the RNA ribose (Uesugi et al., 1979; Guschlbauer & Jankowski, 1980), but is much bulkier and very different in chemical properties. The effect of single and double 2′-*O*-methyluridine substitution in the RNA strand on the NCS-chrom-mediated damage of the RNA·DNA hybrids can be due to the inability of the drug to bind in a ds mode at a particular site (or to bind in the right configuration). The bulky 2′-*O*-methyl substituent might adversely affect the binding but not interfere with the hydrogen abstraction process per se, since the drug-mediated damage at both the RNA and the DNA oligonucleotide strands is significantly affected. Thus, the selectivity in drug binding caused by the 2′-*O*-methyl substitution enables us to identify the abasic site in the RNA oligonucleotide and to relate the abasic site with the cleavage site.

Chemistry of RNA Oligonucleotide Damage. The chemistry of DNA damage by NCS-chrom has been well-studied (Scheme 2). In DNA damage the formation of an abasic site involves 1′ chemistry to form a deoxyribonolactone or 4′ chemistry to form a 4′-hydroxylated abasic site. Since **11a** is relatively stable to isolation (lane 1, Figure 5A) and moves significantly faster than R11, it is suggested that formation of the ribonic acid (ring-opened form of the ribonolactone) via 1′ chemistry is more likely. In light of earlier work that conclusively demonstrated the involvement of 1′ chemistry in NCS-induced DNA damage at certain sites by finding a substantial deuterium isotope effect (Kappen et al., 1990), the 3′-^{32}P-end-labeled R11 containing deuterium at the C-1′ position of the U_8 residue or both the U_8 and U_9 residues was treated with glutathione-activated NCS-chrom. As shown in Figure 9, the substitution of deuterium for protium at C-1′ of U_8 (lanes 2 and 8) or both U_8 and U_9 (lanes 1 and 7) results in significant isotope-induced inhibition of cleavage and **11a** (abasic site) formation. The data in Table 1 show an overall isotope effect of about 3.0.

The observed C1′-^{2}H isotope effect confirms 1′ chemistry and leads us to propose a possible 1′ chemistry mechanism for the NCS-chrom-mediated damage of the RNA oligo-

Table 1: Deuterium Isotope Effect on U Site Damage by NCS-Chrom

experiment 1[a]	$^1H/^2H$[c]	$^1H/^2H$[d]	experiment 2[b]	$^1H/^2H$[c]	$^1H/^2H$[d]
abasic site		3.05	abasic site		3.01
U_8	2.95	2.94	U_8	3.24	3.10
U_9		2.83	U_9		3.08

[a] Glutathione was added last (see lanes 1−6, Figure 9). [b] NCS−chrom was added last (see lanes 7−12, Figure 9). [c] Determined by treatment of CACAGAAUUCG$^{32}_{p}$C and CACAGAAU*UCG$^{32}_{p}$C (U*, 1′-^{2}H) with NCS-chrom (data were quantified by normalization to the band indicated by arrow, see Figure 9). [d] Determined by treatment of CACAGAAUUCG$^{32}_{p}$C and CACAGAAU*U*CG$^{32}_{p}$C (U*, 1′-^{2}H) with NCS-chrom (data were quantified by normalization to the band indicated by arrow, see Figure 9).

Scheme 3: Proposed 1′ Chemistry Mechanism of NCS-Chrom-Mediated Damage on RNA Strand

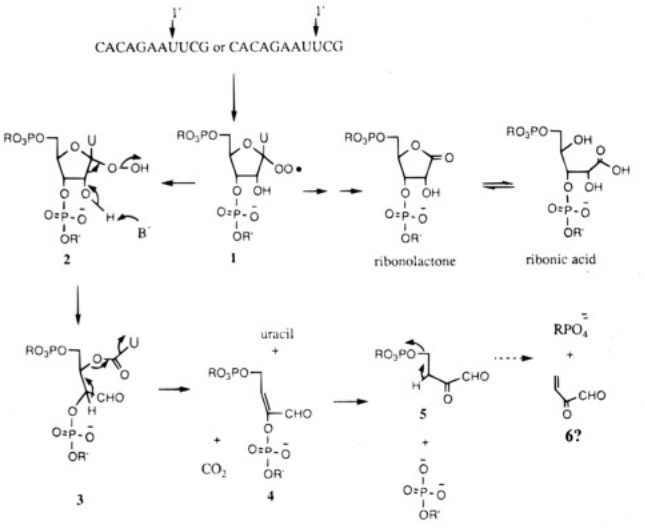

nucleotide strand. As shown in Scheme 3, the abstraction of a hydrogen from C-1′ of ribose to form the ribonic acid is analogous to the 1′ chemistry in DNA damage (Scheme 2). The formation of the cleavage product is proposed to involve the generation of **3** from the putative hydroperoxynucleotide (**2**) via base-catalyzed cleavage of the β-hydroxy peroxide [Giese et al. (1995) and references therein]. Duff et al. (1993) proposed the formation of intermediates **3** from **2** via a Criegee-type rearrangement in the case of C-1′ hydrogen abstraction by Fe−bleomycin from a single ribonucleotide in an oligodeoxynucleotide. However, the Criegee-type mechanism is unlikely to occur for NCS-chrom-mediated damage due to the absence of metal in the reaction or of acidic conditions. Following β-elimination of **3**, the enol phosphate **4** is formed, and the hydrolysis of **4** causes strand cleavage. The smear of radioactivity found upon gel electrophoresis of drug-treated 5′-^{32}P-end-labeled RNA may have resulted from the formation of **5**, which would not be expected to be stable and would degrade during electrophoresis to generate the 3′-phosphate-ended fragment. The complementary DNA strand damage appears to be due to C-5′ chemistry, since all of the cleavage at T_6 and T_7 is 3′-phosphate-ended (comigrating with sequencing marker, see lane 3, Figure 7B). Abasic site formation on the DNA strand caused by 1′ or 4′ chemistry cannot be significant.

Damage of the DNA·DNA Duplex. It was of particular interest to compare the DNA·RNA hybrid reaction, involving virtually entirely 1′ chemistry on the RNA strand, with the DNA·DNA duplex reaction. Figure 10 shows the NCS-chrom-mediated cleavage of the DNA analogue of R11 ^{32}P-end-labeled at the 5′ or 3′ terminus. There is no evidence for the faster moving abasic site band with intact phosphodiester linkages, unlike for the RNA substrate. As shown in Figure 10A, the T site cleavages (lane 2) are 3′-phosphate-ended (the same mobility as the sequencing marker), implicating 5′ chemistry. Previously it had been shown that the 4′-hydroxylated abasic site reacts with hydrazine to form a 3′-phosphopyridazine derivative that moves slower than the corresponding sequencing marker and that the abasic site formed by 1′ or 4′ chemistry can be detected by piperidine-induced enhancement of cleavage (Kappen et al., 1991; Kappen & Goldberg, 1992). There is no obvious abasic site formation for this DNA analogue, as determined by either the hydrazine (lane 3, no 3′-phosphopyridazine formation) or piperidine treatments (lane 4). The likely 5′ chemistry was confirmed in experiments using 3′-end-labeled DNA by the formation of nucleoside 5′-aldehyde (asterisks in lane 2, Figure 10B) that can be reduced by sodium borohydride to the nucleoside (asterisks in lane 3, Figure 10B), oxidized by hypoiodite to the carboxylic acid (asterisks in lane 4, Figure 10B), and further fragmented to the 5′-phosphate-ended fragment by piperidine treatment (asterisks in lane 5, Figure 10B). Thus, while attack at the U residues on the RNA strand involves 1′ chemistry, that on its DNA analogue strand clearly uses 5′ chemistry. Further, it appears that with duplex DNA 5′ chemistry is involved with damage to both strands, whereas in the hybrid 5′ chemistry is limited to the DNA strand. Although it seems likely that this difference in attack site chemistry is due to the A-type conformation of the hybrid, as opposed to the B-type conformation of the DNA duplex, these experiments do not exclude the possibility

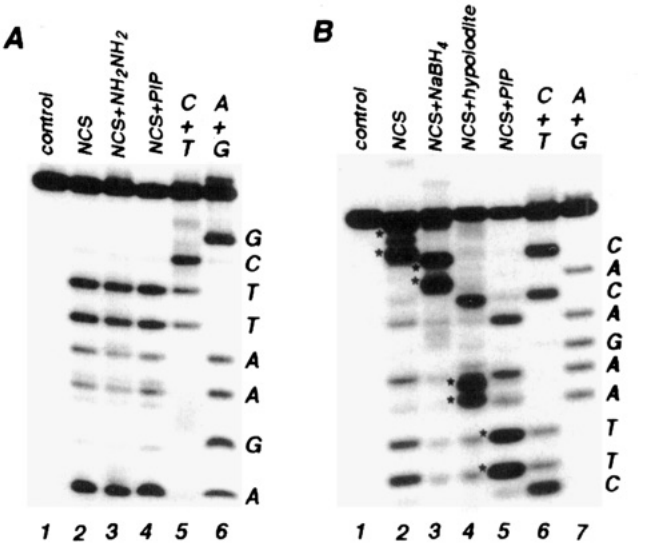

FIGURE 10: NCS-chrom-mediated cleavage of DNA·DNA duplex. NCS-chrom reactions contain CACAGAATTCG (34 μM nucleotide, its complementary strand (76 μM nucleotide), 1 mM glutathione, and 37 μM NCS-chrom. (A) 5′-^{33}P-end-labeled CACAGAATTCG was treated with NCS-chrom (lane 2) and then with hydrazine (lane 3) or piperidine (PIP) (lane 4) as described in Materials and Methods: lane 1, no NCS-chrom control; lanes 5 and 6, Maxam−Gilbert sequencing, C+T and G+A, respectively. (B) 3′-^{33}P-end-labeled CACAGAATTVG$^{32}_{p}$C was treated with NCS-chrom (lane 2) and then with $NaBH_4$ (lane 3) or hypoiodite (lane 4) or piperidine (PIP) (lane 5) as described in Materials and Methods: lane 1, no NCS-chrom control; lanes 6 and 7, Maxam−Gilbert sequencing, C+T and G+A, respectively. Asterisks are explained in the text.

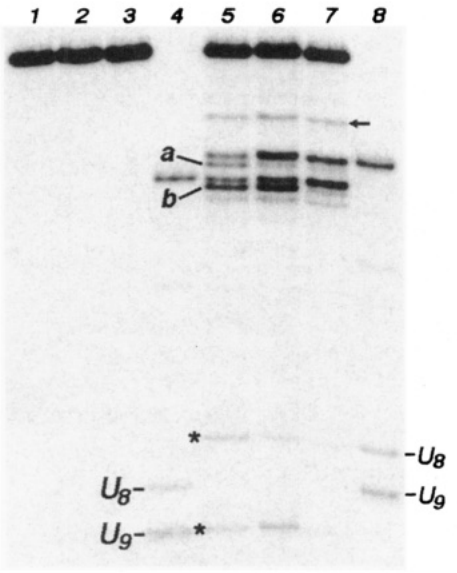

FIGURE 11: NCS-chrom-mediated cleavage of hairpin RNA·DNA oligonucleotide and the effect of deuterium isotope at U residue(s) on the cleavage. Internally ^{32}P-labeled hairpin r(CACAGAAUUCG$_{32p}$)d(TTTTCGAATTCTGTG$_p$) (28 μM nucleotide) was treated with 21 μM NCS-chrom in the presence of 1 mM glutathione (lane 5): lane 6, $\underline{U}_8$* (1′-^{2}H); lane 7, $\underline{U}_8$* (1′-^{2}H) and $\underline{U}_9$* (1′-^{2}H); lanes 1−3, no NCS-chrom controls for lanes 5−7; lanes 4 and 8 U markers from chemical sequencing of synthetic r(CACAGAAUUCG$_{32p}$)d(TTTTCGAA$_p$) and r(CACAGAAUUCG$_{32p}$)d(TTTTCGAAT$_p$), respectively. Arrow indicates the band taken for the normalization of data in different lanes for calculation of the isotope effect. Bands marked a and b are cleavage fragments of the hairpin oligomer containing abasic sites at U_8 and U_9, respectively (see Figure 12). Asteriks designate fragments of ds cleavage of the hairpin oligomer (R_3D_9 and R_2D_8, see Figure 12).

that the difference in the attacked nucleotide (U vs T) accounts for this result.

Damage of Hairpin RNA·DNA Oligonucleotide and Detection of Two ds Cleavage Sites. In order to prove conclusively that the lesions on each strand of the DNA·-RNA hybrid belong primarily to ds lesions, we have used a hairpin substrate composed of hybrid molecules connected by a four-nucleotide linker. A related methodology has recently been used to study ds lesion formation by bleomycin (Absalom et al., 1995). The NCS-chrom-mediated cleavage of the RNA·DNA oligonucleotide containing an internal ^{32}P-phosphodiestesr label is shown in lane 5 of Figure 11. The two ds cleavage sites are explained in Figure 12. The two ss cleavages ($R_{11}D_9$ and $R_{11}D_8$) can be identified by their identical mobility with synthesized marker fragments in lanes 4 and 8. Bands a and b, with slightly faster mobilities, are formed by two ds lesions containing abasic sites at U_8 and U_9, respectively, as identified by the deuterium isotope effect in lane 6, where band a is weaker when U_8 contains 1′-^{2}H, and in lane 7 where both bands a and b are weaker since both U_8 and U_9 contain 1′-^{2}H. The two ds cleavages marked by asterisks can be identified by their mobilities in comparison with the U marker in lanes 4 and 8 and the isotope effect in lanes 6 and 7. The overall isotope effect for ds cleavage is 3.2 ± 0.4. It should be noted that the two ss cleavages in lane 7 are stronger than that in lane 5, indicating that additional ss cleavage at the T site resulted from the ds binding mode due to the expected isotope effect at the U site but not at the T site.

CONCLUDING REMARKS

This study clearly demonstrates that a DNA·RNA hybrid is a substrate for NCS-chrom-induced damage. This reaction resembles that with duplex DNA, in contrast to that with bulged DNA, in that a thiol is required to generate the appropriate diradical reactive species. Further, the damage produced is primarily bistranded. The chemistry involved in the damage on the RNA strand of the hybrid appears to be limited to C-1′ hydrogen abstraction and contrasts with the C-5′ chemistry that occurs at the analogous site of a DNA·DNA duplex. This difference in chemistry may be due to the wider minor groove in the A-type hybrid than in the B-type DNA duplex. On the other hand, the lesion on the complementary DNA strand appears to involve primarily C-5′ hydrogen abstraction for both the hybrid and DNA duplex. It is of interest that no damage was observed in the RNA strand of a DNA·RNA hybrid treated with bleomycin (Krishnamoorthy et al., 1988), although evidence for C-1′ hydrogen abstraction by bleomycin has recently been found at a single ribonucleoside site in an otherwise self-

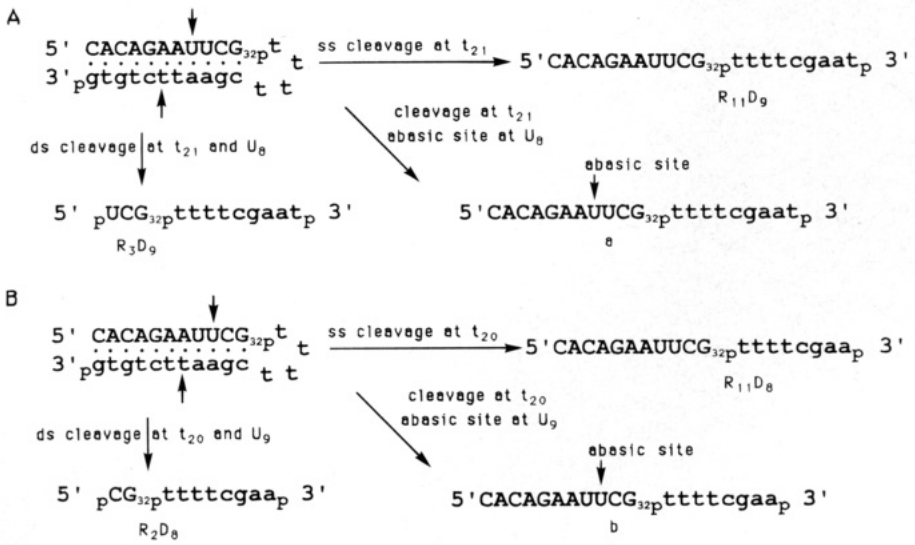

FIGURE 12: Cleavage products generated from NCS-chrom-treated hairpin RNA·DNA oligonucleotide containing internal ^{32}P-phosphodiester label: RNA oligonucleotide, upper case; DNA oligonucleotide, lower case. (A) Single-strand (ss) and double-strand (ds) damage at t_{21} and U_8. (B) Single-strand (ss) and double-strand (ds) damage at t_{20} and U_9.

complementary oligodeoxynucleotide (Duff et al., 1993).

The main lesion generated on the RNA strand by NCS-chrom is an abasic site; the strand break found at the same U residues is a lesser but discrete lesion and does not appear to be due to spontaneous breakdown of the abasic site. A mechanism for the formation of the strand breaks has been proposed that involves the same hydroperoxy intermediate that serves as a precursor of the abasic site lesion.

The use of a 2′-*O*-methyl substituent on the U residue has been useful in identification of the ds partner site on the DNA strand. Although it remains to be further clarified, it appears that this bulky moiety projecting into the floor of the minor groove of the hybrid sufficiently interferes with drug binding in a very localized region (so as not to influence that at the adjacent nucleotide site) to prevent ds lesion formation. This technique also makes it clear that the damaged RNA strand possesses only a single abasic site per molecule.

REFERENCES

Absalon, M. J., Kozarich, J. W., & Stubbe, J. (1995) *Biochemistry 34*, 2065−2075.

Duff, R. J., de Vroom, E., Geluk, A., & Hecht, S. M. (1993) *J. Am. Chem. Soc. 115*, 3350−3351.

England, T. E., Bruce, A. G., & Uhlenbeck, O. C. (1980) *Methods Enzymol. 65*, 65−74.

Gao, X., Stassinopoulos, A., Gu, J., & Goldberg, I. H. (1995a) *Bioorg. Med. Chem. 3*, 795−809.

Gao, X., Stassinopoulos, A., Rice, J. S., & Goldberg, I. H. (1995b) *Biochemistry 34*, 40−49.

Giese, B., Beyrich-Graf, X., Erdmann, P. Giraud, L., Imwinkelried, P., Müller, S. N., & Schwitter, U. (1995) *J. Am. Chem. Soc. 117*, 6146−6147.

Goldberg, I. H. (1991) *Acc. Chem. Res. 24*, 191−198.

Goldberg, I. H., & Kappen, L. S. (1994) in *Enediyne Antibiotics as Antitumor Agents* (Borders, D. B., & Doyle, T. W., Eds.) pp 327−362, Marcel Dekker, New York and Basel.

Guschlbauer, W., & Jankowski, K. (1980) *Nucleic Acids Res. 8*, 1421−1433.

Hensens, O. D., Helms, G. L., Zink, D. L., Chin, D.-H., Kappen, L. S., & Goldberg, I. H. (1993) *J. Am. Chem. Soc. 115*, 11030−11031.

Hensens, O. D., Chin, D.-H., Stassinopoulos, A., Zink, D. L., Kappen, L. S., & Goldberg, I. H. (1994) *Proc. Natl. Acad. Sci. U.S.A. 91*, 4534−4538.

Herschlag, D., Eckstein, F., & Cech, T. R. (1993) *Biochemistry 32*, 8299−8311.

Kappen, L. S., & Goldberg, I. H. (1983) *Biochemistry 22*, 4872−4878.

Kappen, L. S., & Goldberg, I. H. (1985) *Nucleic Acids Res. 13*, 1637−1648.

Kappen, L. S., & Goldberg, I. H. (1992) *Biochemistry 31*, 9081−9089.

Kappen, L. S., & Goldberg, I. H. (1993a) *Science 261*, 1319−1321.

Kappen, L. S., & Goldberg, I. H. (1993b) *Biochemistry 32*, 13138−13144.

Kappen, L. S., & Goldberg, I. H. (1995) *Biochemistry 34*, 5997−6002.

Kappen, L. S., Chen, C. Q., & Goldberg, I. H. (1988) *Biochemistry 27*, 4331−4878.

Kappen, L. S., Goldberg, I. H., Wu, S. H., Stubbe, J., Worth, L., Jr., & Kozarich, J. W. (1990) *J. Chem. Chem. Soc. 112*, 2797−2798.

Kappen, L. S., Goldberg, I. H., Frank, B. L., Worth, L., Jr., Christner, D. F., Kozarich, W., & Stubbe, J. (1991) *Biochemistry 30*, 2034−2042.

Khare, D., & Orban, J. (1992) *Nucleic Acids Res. 20*, 5131−5136.

Krishnamoorthy, C. R., Vanderwall, D. E., Kozarich, J. W., & Stubbe, J. (1988) *J. Am. Chem. Soc. 110*, 2008−2009.

Milligan, J. F., Groebe, D. R., Withereli, G. W., & Uhlenbeck, O. C. (1987) *Nucleic Acids Res. 15*, 8783−8798.

Peattie, D. A. (1979) *Proc. Natl. Acad. Sci. U.S.A. 76*, 1760−1764.

Poon, R., Beerman, T. A., & Goldberg, I. H. (1977) *Biochemistry 16*, 486−493.

Steinschneider, A., & Fraenkel-Conrat, H. (1966) *Biochemistry 5*, 2735−2743.

Strobel, S. A., & Cech, T. R. (1993) *Biochemistry 32*, 13593−13604.

Uesugi, S., Miki, H., Iwahashi, H., & Kyogoku, Y. (1979) *Tetrahedron Lett. 42*, 4073−4076.

Vorbrüggen, H., & Bennua, B. (1981) *Chem. Ber. 114*, 1279−1286.

BI951474R